

Continuous Plantar Pressure Modeling Using Sparse Sensors

Sarah Ostadabbas, Mehrdad Nourani
Department of Electrical Engineering
University of Texas at Dallas, Richardson, TX 75080
{sarahostad, nourani}@utdallas.edu

Matthew Pompeo, M.D.
Presbyterian Wound Care Clinic
Dallas, TX 75231
healerone@aol.com

Abstract—The foot complications constitute a tremendous challenge for diabetic patients, caregivers, and the healthcare system. With current technology, in-shoe monitoring systems can be implemented to continuously monitor foot's at-risk ulceration sites and send feedback to patients and physicians. The few available high resolution in-shoe pressure measuring systems are extremely expensive and targeting clinical use only. The more affordable price ranges can be reached by limiting the number of sensors in the shoe. Precise subject-specific sensor placement is still a challenge in such platforms. Moreover, there is no good way to estimate pressure on other points of the foot. In this paper, we address these technical challenges by proposing SCPM algorithm that reconstructs a continuous foot plantar pressure image from a sparse set of sensor readings. Using our technique, sensor placement can be the same in every electronic insole. However, the SCPM's trained parameters are unique for every subject and foot.

Index Terms—Continuous Image Reconstruction, Diabetic Foot Ulcers, In-shoe Pressure Monitoring, Plantar Pressure Modeling.

I. INTRODUCTION

A. Motivation

According to the American Diabetes Association (ADA), about 25.8 million people in the United States suffer from diabetes [1]. Up to 25% of diabetic individuals will develop a foot ulcer during their lifetime [2]. Of these people, 12% to 24% eventually must undergo amputation as a result of infection due to the foot ulcer [3]. Any reduction in the rate of diabetic foot complications would be significant to healthcare providers, and more importantly, would improve the quality of life for many individuals.

Diabetes over time can damage the nervous system and cause neuropathy. A patient with neuropathy is not able to feel his or her feet properly to allow the traumatized foot to recover [4]. With current technology, electronic pressure monitoring systems can be placed as insoles into normal shoes to continuously monitor at-risk ulceration sites of foot and give early warning/feedback to patients and physicians.

B. Related Works

Several systems for measuring high resolution plantar pressure of foot are commercially available. Among these are the Pedar [5], F-Scan [6] and Parotec [7]. These systems are extremely expensive (order of \$10k–\$20k in 2012 models) and mostly aim at athletic foot/running or clinical analysis.

For such a system to be affordable to regular patients, it would need to be at a much lower price. This price point can be reached primarily by limiting the number of sensors in the shoes. An early foot-to-ground force measurement device was reported by Spolek and Lippert in 1976 [8]. The system was restricted to measure heel and toe forces during several steps. Wertsch et. al. presented a portable plantar pressure measurement system with seven sensors located under high risk area of foot [9]. The more recent studies aimed at more in-situ processing ability by using a computing device/gateway attached to the waist [10–12].

In all of these system, a limited number of sensors are mounted on a few regions of foot plantar area. These regions are selected and fixed based on either the medically-predefined high risk ulceration sites of foot [12], or foot pressure image obtained from a pressure indicating film while subject standing on it [10]. The main draw back of these systems is except for a few exact points under the sensors, pressure distribution information on other points of plantar area is completely lost. Moreover, plantar pressure distribution based on foot shapes and existing deformities is very subject-specific. So, sensor placements should be carefully adjusted for every patients, and even for a given subject, exact sensor placement is critical to capture accurate data. Therefore, finding sensor placements remained as a research problem and did not become practical for widely-used reasonable-priced electronic insoles.

Plantar pressure modeling can be used as a method to estimate the foot pressure distribution all over plantar area for each individual by using limited number of parameters. Foot modeling in diabetes research are mainly offered in two categories. First, Finite Element (FE) approaches to model foot mechanical structure and tissue characteristics [13]. These models can be used to predict the effect of accommodative in-shoe orthoses or insoles. The complexity of this approach prevents its real-time applications. Second, various mathematical modeling methods to extract relevant features for different classification purposes. Authors in [14] applied Principal Component Analysis (PCA) on dynamic foot pressure image to extract eigenvalues as features and used a Fuzzy classifier to distinguish normal and diabetic subjects. In this line of research, models are not used to predict more detailed data, but only used for classification.

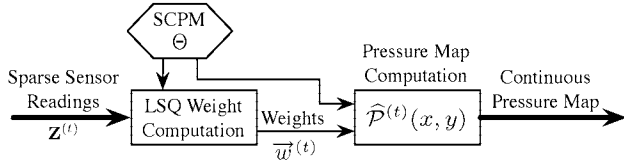


Fig. 1. Generating continuous pressure map using SCPM

C. Key Contribution

To deal with the problems of pressure measurement systems with limited number of sensors, a method to model the pressure distribution all over the plantar area is presented in this paper. Our proposed Sparse sensing Continuous Plantar pressure Model (SCPM) is developed such that by using sparse number of pressure sensors a continuous image of foot plantar pressure can be reconstructed during walking.

Patient-specific parameters of this model can be tuned during patient clinical visit by performing a short software training phase. In training phase, patients are asked to walk on a high resolution pressure mat and the pressure data is used to create an accurate foot pressure model of the patients. In our technique, sensor placement can be the same in every electronic insole, but the SCPM is unique for every subject and foot.

II. SPARSE SENSING CONTINUOUS PLANTAR PRESSURE MODEL (SCPM)

The foot has a number of key points of contact with the ground/shoe based on bone structure and walking patterns. In each step, the weight shifts among these contact points and between two feet. Many in-shoe monitoring systems depend on pressure sensors placed precisely at these pressure points. There are several problems with this method: a) the pressure sensors have to be uniquely placed for each subject, b) small misplacement greatly affects accuracy, and c) there is no good way to estimate pressure on other points on the foot.

A. Model Overview

In this paper, we model the foot pressure distribution by using a sparse set of sensor readings called Sparse sensing Continuous Plantar pressure Model (SCPM). This model uses a modified Gaussian Mixture Model (GMM) to reconstruct a continuous plantar pressure map. In the SCPM, each pressure point is represented by one or more Gaussian functions. Gaussians were chosen since GMMs are among the most statistically mature methods for clustering and density estimation [15]. The number of Gaussians, their centers, and their covariance (shape) are trained using data from a high resolution pressure mapping system.

SCPM is unique for every subject and foot. After training, a sparse set of sensor readings can be used to estimate the weights (amplitudes) of each Gaussian using a least squares (LSQ) method. The pressure can be estimated anywhere on the foot by summing the weighted contributions of each Gaussian.

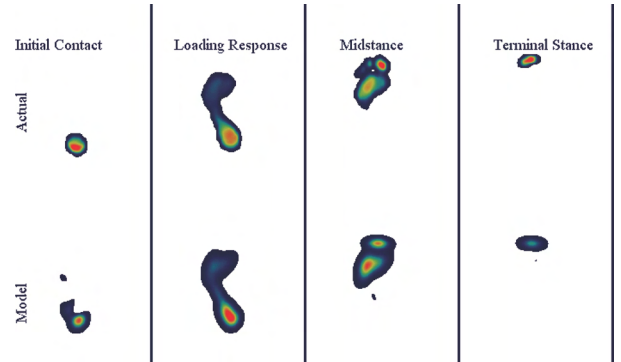


Fig. 2. Actual and reconstructed model for different phases of step

An overview of SCPM that generates a continuous pressure map is illustrated in Fig. 1. The reconstructed sensor image is compared with the actual image for several spots in the gait cycle for a single step and subject in Fig. 2. This figure was made from a $K = 10$ SCPM with full covariance matrices as explained in Section III.

The SCPM takes advantage of high resolution pressure data during training to create an accurate pressure model of the subject's foot. Subsequently, only a small number of sensors is required to estimate pressure anywhere on the foot. Furthermore, the sensors do not need to be placed on exact peak pressure areas to generate an accurate map. This allows mass production of generic sensor insoles rather than the per-subject customization required for other methods. While high resolution pressure mapping systems are too expensive for individual's at-home use, they can be affordably used in-office to generate the pressure model during training phase.

B. Computing Pressure Map

The SCPM models plantar pressure with a compact set of K basis functions. In this model, plantar pressure at time t is represented by the finite pressure weight vector $\vec{w}^{(t)} = [w_1^{(t)}, \dots, w_K^{(t)}]$. From this vector, an estimate of the plantar pressure, $\mathcal{P}^{(t)}$, at coordinate $\langle x, y \rangle$ at time t is obtained as follows:

$$\hat{\mathcal{P}}^{(t)}(x, y) = \sum_{i=1}^K w_i^{(t)} F(x, y, \Theta_i) \quad (1)$$

$F(\cdot)$ is a function of pressure point coordinate, x , y , and the model parameters, Θ . Any continuous function, F , can be used, although in this paper, Gaussians are considered exclusively. The model must be trained uniquely for each subject and foot to extract parameter Θ .

C. LSQ Weight Computation

Once trained, the pressure weight vector, $\vec{w}^{(t)}$, can be estimated using LSQ algorithm from a set of observations, $\mathbf{Z}^{(t)}$. Each observation, z_j in $\mathbf{Z}^{(t)} = \{z_1, z_2, \dots, z_N\}$, is a 3-tuple containing the coordinate and pressure value at time t : $z_j = (x_j, y_j, \mathcal{P}_j)$.

Using $\mathbf{Z}^{(t)}$ and Eqn. (1), we can now generate a system of linear equations at each time frame (for simplicity, the superscript (t) is eliminated):

$$\begin{aligned} \sum_{i=1}^K w_i F(x_1, y_1, \Theta_i) &= \mathcal{P}_1 \\ \sum_{i=1}^K w_i F(x_2, y_2, \Theta_i) &= \mathcal{P}_2 \\ \vdots & \\ \sum_{i=1}^K w_i F(x_N, y_N, \Theta_i) &= \mathcal{P}_N \end{aligned} \quad (2)$$

In general, if the number of observations is greater than the number of basis functions ($N > K$), the pressure weight vector would need to be estimated with the LSQ approach [16]. Let's define matrix \mathbf{A} with $A_{ij} = F(x_j, y_j, \Theta_i)$ as elements. Eqn. (2) can now be converted to $\mathbf{A}\vec{w} = \vec{\mathcal{P}}$. By applying the technique of linear least squares, we get:

$$\vec{w} = (\mathbf{A}^T \mathbf{A})^{-1} \mathbf{A}^T \vec{\mathcal{P}} \quad (3)$$

Once the pressure weight vector is found for a sampling frame, as shown in Fig. 1, the continuous plantar pressure map can be estimated using Eqn. (1).

III. SCPM TRAINING PROCEDURE

SCPM is able to reconstruct a spatially-continuous map of the foot pressure from spatially sparse sensor data. This is achieved by using basis functions to approximate the pressure distribution from a small number of contact points. Choosing the basis function parameters that best describe a particular foot requires high resolution pressure data from that subject. The training process uses that data to choose the model parameters, Θ , to maximize fit according to some objective function.

Prior to training, the data has to be preprocessed. The preprocessing consists of splitting each subject's walking data into steps and then aligning the individual steps (translation and rotation). Every frame in a step is considered to have the same alignment—once the subject's foot touches the ground, the subject does not slide or rotate the foot. After this preprocessing, the parameters are trained using a modified Expectation Maximization (EM) as formulated for mixture models [17]. An overview of the SCPM per-subject training procedure is shown in Fig. 3. The preprocessing and training steps are described in this section. After presenting a generalized model, we look at the specific details when using Gaussians for the basis function.

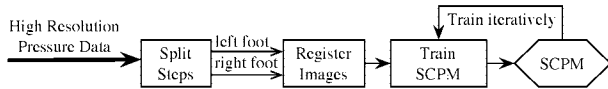


Fig. 3. SCPM per-subject training procedure

A. Step Splitting

The two aspects to step splitting are a) differentiating between one step and the next, and b) determining whether the step is a right step or left step. The pressure mat used for this research [6], only had room enough for one foot, so subjects were instructed to walk three steps in one direction, turn around, and walk three steps in the opposite direction. Only the middle step was recorded, and subjects were instructed to alternate between right and left foot when touching the mat.

Once a step started, there was always some pressure recorded on the pressure mat until the step finished, followed by some period with no pressure recorded until the next step began. The steps were separated based on these zero-pressure intervals. The steps were then split into odd steps (left foot) and even steps (right foot).

B. Image Registration

In order to align the foot pressure image of different steps, the first walking step in each set of steps was used as the registration template for each subject and foot. The image registration algorithm is a modified version of the methods presented in [18, 19] with the following steps:

- 1) **Create Peak Pressure Image (PPI):** Each pixel of PPI holds the maximum pressure value on that spatial coordinate among all frames in a given step.
- 2) **Rotational Alignment:** The PPI is test-rotated by each of several evenly spaced angles over an initial window of 360° . The rotated PPI is translationally aligned (as described in step 3). The alignment with the lowest Root Mean Square (RMS) error between the template and step PPIs is saved.
- 3) **Translational Alignment:** Translation in the space-domain corresponds to a phase shift in the frequency-domain. Spatial translation can be determined by applying two-dimensional Discrete Fourier Transform (DFT) on the PPIs to measure the shift between each PPI and the template.
- 4) **Iteratively Converge:** The angular window from step 2 is shrunk by a constant factor and centered on the saved alignment. Steps 2 and 3 are applied iteratively until alignment precision is sufficient, such that the angle difference between this iteration and the previous one becomes less than ϵ .

C. Training SCPM with EM

The model parameters are trained using an EM process. As SCPM is derived from the GMM, it's important to highlight some of the differences. The key difference is that SCPM is used for curve-fitting or interpolation, while a GMM is a probability distribution.

- **Basis function weights can sum to a number other than 1** Probability distribution functions must integrate to 1. Since the component functions in a mixture model have this property, as long as the weights sum to 1, this is maintained. The SCPM has no such limitation, either for the basis functions or the weights.

- **Value associated with each observation** In a traditional GMM, each observation only has a coordinate, but no value. For the SCPM, each observation has a coordinate and an associated pressure. The EM algorithm can be adopted by assigning a weight to each observation equal to the pressure. These weights are different than the basis function weights [20].
- **Basis function weights calculated per frame, other parameters per-foot** This is equivalent to saying that there is a separate mixture model for each frame with the basis function parameters tied across all frames from the same subject and foot [21].

Our generalized EM training algorithm is shown in Algorithm. 1. On line 3, the parameters are randomly initialized based on the observations. For this work, the center of each Gaussian, μ , was randomly selected among the observation coordinates, and the covariance matrix was set to a fixed value.

During the expectation phase, the basis function membership (Ω) is calculated for each observation. This value represents the contribution from a particular basis function to the value of the observation. $\mathbf{Z}_{wi}^{(t)}$ holds the per-frame weighted observations (where the pressure is weighted by the set membership) for calculating the frame weight of the basis function (line 20). These per-frame weighted observations combine to form \mathbf{Z}_{wi} , the weighted observations. These weighted observations are used to calculate the optimal fit of basis function i for $i = 1 \rightarrow K$.

The function $G(\mathbf{Z}_{wi})$ maximizes the fit of the basis function i to the weighted observations according to some objective function. For this paper, Gaussian functions are used with maximum likelihood criteria used in [15].

D. Gaussians as Basis Functions

GMM is a weighted sum of K component Gaussian densities that can be served as the continuous basis functions in SCPM. Each component density, $g(\cdot)$, is a D -variate Gaussian function of the form:

$$g(\mathcal{X}, \mu_i, \Sigma_i) = \frac{1}{(2\pi)^{D/2} |\Sigma_i|^{1/2}} e^{(-\frac{1}{2}(\mathcal{X} - \mu_i)^T \Sigma_i^{-1} (\mathcal{X} - \mu_i))} \quad (4)$$

where \mathcal{X} is a D -dimensional continuous-valued data vector with mean vector μ_i and covariance matrix Σ_i [22].

To adapt the Gaussian density to the SCPM, the model parameters would be $\Theta_i = \{\mu_i, \Sigma_i\}$, and \mathcal{X} corresponds to a 2-dimensional coordinate data $\langle x, y \rangle$. In our case, the mean vector and covariance matrix of coordinate data will be:

$$\mathcal{X} = \begin{pmatrix} x \\ y \end{pmatrix}, \quad \mu = \begin{pmatrix} \mu_x \\ \mu_y \end{pmatrix}, \quad \Sigma = \begin{pmatrix} \sigma_x^2 & \rho\sigma_x\sigma_y \\ \rho\sigma_x\sigma_y & \sigma_y^2 \end{pmatrix} \quad (5)$$

where ρ is the correlation between coordinate vector, x and y .

In general, the geometric interpretation of a Gaussian distribution is an ellipsoid centered at the mean. For a given model, the covariance matrix, Σ can be forced to have a specific structure. The three common types are “full”, “diagonal”, and

Algorithm 1 Expectation-Maximization

```

1: {=== Initialize Parameters ===}
2: for  $i = 1 \rightarrow K$  do {For each basis function}
3:    $\Theta_i \leftarrow \text{randInit}(\mathbf{Z})$  {Randomly initialize parameters}
4:   for  $t = 1 \rightarrow T$  do {For each frame}
5:      $w_i^{(t)} \leftarrow 1$  {Initialize weights to 1}
6:   end for
7: end for
8: {=== Main Algorithm ===}
9: for  $m = 1 \rightarrow M$  do {For each training iteration}
10:  for  $i = 1 \rightarrow K$  do {For each basis function}
11:     $\mathbf{Z}_{wi} \leftarrow \emptyset$  {Initialize weighted observation data}
12:    for  $t = 1 \rightarrow T$  do {For each frame}
13:       $\mathbf{Z}_{wi}^{(t)} \leftarrow \emptyset$ 
14:      for all  $(x, y, \mathcal{P}) \in \mathbf{Z}^{(t)}$  do {For each sample}
15:        {Expectation: per-point function membership}
16:
17:          $\Omega \leftarrow \frac{w_i^{(t)} F(x, y, \Theta_i)}{\sum_{k=1}^K w_k^{(t)} F(x, y, \Theta_k)}$ 
18:          $\mathbf{Z}_{wi}^{(t)} \leftarrow \mathbf{Z}_{wi}^{(t)} \cup \{(x, y, \Omega)\}$ 
19:       end for
20:       {Maximization: Weights}
21:        $w_i^{(t)} \leftarrow \frac{1}{\|\mathbf{Z}\|} \sum_{(x, y, \mathcal{P}) \in \mathbf{Z}_{wi}^{(t)}} \mathcal{P}$ 
22:        $\mathbf{Z}_{wi} \leftarrow \mathbf{Z}_{wi} \cup \mathbf{Z}_{wi}^{(t)}$ 
23:     end for
24:     {Maximization: Basis function parameters}
25:      $\Theta_i \leftarrow G(\mathbf{Z}_{wi})$ 
26:   end for

```

“equal” covariance matrices. A full covariance matrix can be an ellipsoid rotated at any angle. A diagonal covariance matrix has $\rho = 0$ which results in an ellipsoid aligned to the x or y axes. Finally, an equal matrix is a diagonal matrix with both elements set to the same value. This results in a circle.

IV. EXPERIMENTAL RESULTS

In order to collect pressure data for SCPM training, we use the MatScan pressure measurement system [6]. This floor mat can capture barefoot plantar pressure with 1.4 sensors/cm² density. There were 44 × 52 sensing cells on the pressure mat.

Five healthy subjects including two females, in age range from 20 to 51 years old, were asked to perform the training phase for two minutes and pressure sensor data was sampled at 50 Hz. The high resolution pressure mat was placed in the middle of a 5 meter long walkway and subjects were asked to walk normally across it in one direction, then to turn around and walk in the other direction. Subjects were asked to put the right foot on the mat while walking one direction, and the left foot in the other. The subjects were asked to practice for 1 minute before the test started to ensure proper foot placement and to get them used to the system. 70% of the steps were used for training the model to extract SCPM parameters and

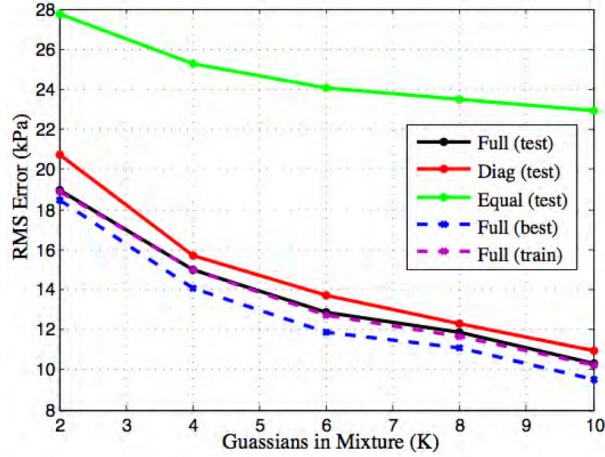


Fig. 4. Per-sensor RMS error across all subjects and trials

the rest used to test the accuracy and efficiency of our proposed algorithm.

In most sampling experiments, the Root Mean Square (RMS)-per sensing cell error is used. This is considered superior to average error as it considers both positive and negative deviations, and it emphasizes the larger errors. Specifically, RMS error is equivalent to:

$$e_{rms}^2 = \bar{e}^2 + \sigma_e^2 \quad (6)$$

where \bar{e} is the arithmetic mean and σ_e is the standard deviation of per-sensor errors.

A. Effect of Number of Gaussians

To show the effect of K , the number of Gaussian mixtures used in our modeling, the accuracy of data reconstruction is evaluated at $K = 2, 4, 6, 8$ and 10 Gaussians. Since the EM algorithm is sensitive to initial value of parameters, for a given K , the parameter estimation was run 5 different times. The RMS model error for different number of Gaussians (K) is shown in Fig. 4. This was evaluated across all sensors covered by the foot and all subjects. The RMS error decreases by adding more degree of freedom to Σ . We consider three different structures for Σ from Eqn. (5): 1) Full: with full degree of freedom, 2) Diag: diagonal matrix by setting $\rho = 0$, and 3) Equal: equal-elements diagonal matrix by setting diagonal with $\rho = 0$, $\sigma_x = \sigma_y$. Also, for a given Σ structure, greater K results in less RMS error. The training and test errors in full Σ structure are almost identical that indicates no overfitting happened in the training phase.

The training model with least RMS error among all 5 trials for each subject was used in test phase and the test RMS modeling error is also shown in Fig. 4 as “Full (best)”. This error is less than all-trial error which indicates the more accurate training model guarantees more accurate test results. As EM is sensitive to initial conditions, it makes sense to train several and select the best. This should also offer greater stability.

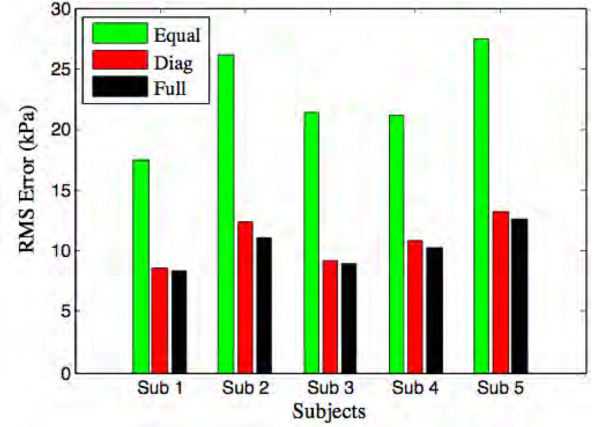


Fig. 5. Per-subject error for 10 Gaussian mixtures

To compare the individual subject’s results, SCPM for $K = 10$ with different Σ structures was computed. The RMS model error in test phase for each subject is shown in Fig. 5. As you can see, the individual’s results follow all-subject results on effect of Σ structure.

B. Effect of Number of Sensors

So far, to reconstruct the plantar pressure image, all sensor data from high resolution mat was used to calculate the optimal values for the pressure weight vector \vec{w} . However, the anticipated application is sensor insole with very few sensors. To study the effect of N , the number of sensors, we randomly choose a subset of pressure sensors from all sensing cell locations and compute the RMS modeling error with them for a SCPM with $K = 10$ and a full covariance matrix as is shown in Fig. 6. For each value of N , 10 different randomly chosen sensor sets were used. Given that no effort was made to select a “good” set, it is not surprising that the error goes high as the sensors become more sparse.

This is addressed in Table I by using exactly $N = K$

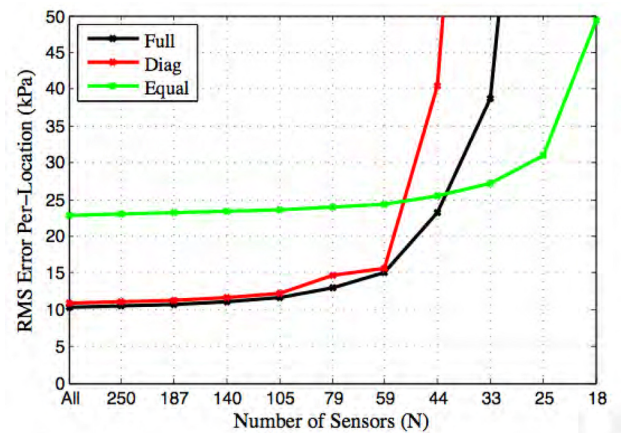


Fig. 6. Per-location error from sparse sensor data

sensors and setting the sensor location to each of the Gaussian centers. This was tested on both the left and right feet for all trained models (not just the best trial). The table clearly shows that even with a small number of basis functions, the error remains low. Certain subjects and values of K show very high error compared with the others. After we investigated, we discovered that for Sub1 and $K = 10$ (which had a reported error of 102 (kPa)), all trials were under 14 kPa except for one, which had 318 kPa error. Because RMS error is biased towards high error, this skewed the results considerably. This result demonstrates that it is important to select the best of the trained models. If we had done this, the few high results would not have been present.

TABLE I
PER-LOCATION RMS ERROR (KPA) FOR SPARSE SENSORS AT GAUSSIAN CENTERS ($N = K$)

Subject	Number of Gaussians/Locations				
	10	8	6	4	2
Sub 1	102.25	13.14	12.71	14.05	17.36
Sub 2	15.80	13.20	12.46	13.47	14.68
Sub 3	22.37	30.33	19.16	20.27	22.84
Sub 4	13.92	14.53	15.84	16.05	19.03
Sub 5	18.27	39.21	18.94	19.84	26.15

V. CONCLUSION

Foot complications are common in diabetic patients and are considered one of the most expensive complications to treat. With current technology, electronic pressure monitoring systems can be placed as an insole into normal shoes to continuously monitor at-risk ulceration sites of foot and give early warning/feedback to patients and physicians. The few available high resolution pressure mapping systems are extremely expensive. For such a system to be affordable to patients, it would need to be at a much better price. This price point can be reached with some compromising: primarily the number of sensors in the shoe would be very limited. Many of these in-shoe monitoring systems depend on precise pressure sensors placement. There are several problems with this method including being subject-specific and not having a good way to estimate pressure on other points on the foot. In this paper, we proposed a novel plantar pressure model, SCPM, that by using sparse number of pressure sensors reconstructs a continuous image of foot plantar pressure uniquely for every subject and foot.

REFERENCES

- [1] American Diabetes Association, <http://www.diabetes.org/>, 2011.
- [2] N. Singh, D. Armstrong, and B. Lipsky, "Preventing foot ulcers in patients with diabetes," *JAMA: the journal of the American Medical Association*, vol. 293, no. 2, pp. 217–228, 2005.
- [3] Stillman RM, "Diabetic ulcers E Medicine," <http://www.emedicine.com/med/topic551.htm>, 2005.
- [4] A. Veves, H. Murray, M. Young, and A. Boulton, "The risk of foot ulceration in diabetic patients with high foot pressure: a prospective study," *Diabetologia*, vol. 35, no. 7, pp. 660–663, 1992.
- [5] Novel USA, "The Pedar System," <http://www.novelusa.com/>, 2012.

- [6] Tekscan, "Pressure Mapping, Force Measurement, and Tactile Sensors," <http://www.tekscan.com/>, 2012.
- [7] The London Orthotic Consultancy (LOC), "Parotec plantar pressure measurement system," <http://www.londonorthotics.co.uk/>, 2012.
- [8] G. Spolek, E. Day, F. Lippert, and G. Kirkpatrick, "Ambulatory-force measurement using an instrumented-shoe system," *Experimental Mechanics*, vol. 15, no. 7, pp. 271–274, 1975.
- [9] J. Wertsch, J. Webster, and W. Tompkins, "A portable insole plantar pressure measurement system," *J Rehabil Res Dev*, vol. 29, no. 1, pp. 13–18, 1992.
- [10] Z. Abu-Faraj, G. Harris, J. Abler, and J. Wertsch, "A holter-type, microprocessor-based, rehabilitation instrument for acquisition and storage of plantar pressure data," *Journal of rehabilitation research and development*, vol. 34, pp. 187–194, 1997.
- [11] S. Walker, P. Helm, and L. Lavery, "Gait pattern alteration by functional sensory substitution in healthy subjects and in diabetic subjects with peripheral neuropathy," *Archives of physical medicine and rehabilitation*, vol. 78, no. 8, pp. 853–856, 1997.
- [12] Z. Pataky, L. Faravel, J. Da Silva, and J. Assal, "A new ambulatory foot pressure device for patients with sensory impairment. a system for continuous measurement of plantar pressure and a feed-back alarm," *Journal of biomechanics*, vol. 33, no. 9, pp. 1135–1138, 2000.
- [13] D. Lemmon, T. Shiang, A. Hashmi, J. Ulbrecht, and P. Cavanagh, "The effect of insoles in therapeutic footwear—a finite element approach," *Journal of Biomechanics*, vol. 30, no. 6, pp. 615–620, 1997.
- [14] U. Acharya, J. Tong, V. Subbhuraam, C. Chua, T. Ha, D. Ghista, S. Chattopadhyay, K. Ng, and J. Suri, "Computer-based identification of type 2 diabetic subjects with and without neuropathy using dynamic planter pressure and principal component analysis," *Journal of medical systems*, pp. 1–9, 2011.
- [15] J. Bilmes, "A gentle tutorial of the em algorithm and its application to parameter estimation for gaussian mixture and hidden markov models," 1998.
- [16] C. Lawson and R. Hanson, "Solving least squares problems," vol. 15, 1995.
- [17] G. McLachlan and T. Krishnan, "The em algorithm and extensions," vol. 274, 1997.
- [18] F. Oliveira, T. Pataky, and J. Tavares, "Registration of pedobarographic image data in the frequency domain," *Computer Methods in Biomechanics and Biomedical Engineering*, vol. 13, no. 6, pp. 731–740, 2010.
- [19] F. Oliveira, A. Sousa, R. Santos, and J. Tavares, "Spatio-temporal alignment of pedobarographic image sequences," *Medical and Biological Engineering and Computing*, pp. 1–8, 2011.
- [20] D. Reynolds, T. Quatieri, and R. Dunn, "Speaker verification using adapted gaussian mixture models," *Digital signal processing*, vol. 10, no. 1-3, pp. 19–41, 2000.
- [21] S. Young, "The general use of tying in phoneme-based hmm speech recognisers," in *Acoustics, Speech, and Signal Processing, ICASSP-92. IEEE International Conference on*, vol. 1. IEEE, 1992, pp. 569–572.
- [22] D. Reynolds, "Gaussian mixture models," *Encyclopedia of Biometric Recognition*, 2008.